Geoderma 451 (2024) 117082

Contents lists available at ScienceDirect

Geoderma

journal homepage: www.elsevier.com/locate/geoderma

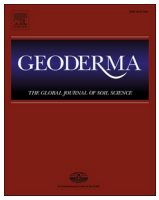

Adsorption of extracellular enzymes by biochar: Impacts of enzyme and biochar properties

Lingqun Zeng [a], Andrew R. Zimmerman [b], Rixiang Huang [a,*]

[a] Department of Environmental and Sustainable Engineering, University at Albany, Albany, NY 12222, United States
[b] Department of Geological Sciences, University of Florida, Gainesville, FL 32611, United States

ARTICLE INFO

Handling Editor: M. Cayuela

Keywords:
Extracellular enzymes
Pyrogenic carbon
Biochar
Adsorption
Carbon cycling
Soil health

ABSTRACT

Extracellular enzymes play a key role in mediating organic matter decomposition in soils and the mobility of enzymes is largely controlled by their interaction with soil surfaces. The introduction of pyrogenic products, including biochar produced for the purpose of carbon sequestration or soil health management, may alter the ecological functioning of soil. In this work, we studied the adsorption of four representative soil extracellular enzymes (urease, invertase, α-amylase and protease) to biochar (derived from wood biomass and wheat straw produced at different pyrolysis temperatures, and a wildfire pine char) and soil mixed with biochar. A pH-edge adsorption experiment showed that, for all biochar/enzyme combinations, adsorption of all extracellular enzymes decreased as pH increased from 4 to 9. This pH dependency suggests that electrostatic interaction was the primary adsorption mechanism. Equilibrium enzyme adsorption data was best fit by the Langmuir isotherm and adsorption capacity varied significantly with enzyme type, ranging from 67 to 232 $mg{\cdot}g^{-1}$ for urease and 0 to 11 $mg{\cdot}g^{-1}$ for the others at pH 5.0. Enzyme adsorption also differed among biochars with or without surface oxidation treatment. Correlations between enzyme adsorption data and biochar properties demonstrated the relevance of enzyme sizes, biochar surface porous structure, and surface chemical functionality in determining biochar adsorption capacity and affinity for enzymes. Soil adsorption experiment showed that biochar addition can enhance or reduce soil adsorption of enzymes, depending on the relative enzyme affinity between the soil and biochar. These findings indicate that pyrogenic organic matter has varying impacts on the mobility of soil extracellular enzymes through direct adsorption and potentially affect the activity and stability of enzymes, and ultimately soil carbon and nutrient cycling.

1. Introduction

Microbial extracellular enzymes play an essential role in soil organic matter (SOM) decomposition, by catalyzing hydrolytic and oxidative reactions that depolymerize complex macromolecules (Burns et al., 2013). Once released extracellularly to soil by microbes, activities of enzyme are affected by soil environmental conditions such as pH, temperature and soil physical components (Allison, 2006; Sinsabaugh et al., 2008; Kaiser et al., 2010). The interactions of enzymes with solid soil components largely determine their accessibility to substrates, their specific catalytic activity, and their activity lifetime (Allison, 2006; Foster et al., 2018).

Pyrogenic carbon (or biochar or black carbon) is a carbonaceous material derived from thermochemical processing of biomass. Pyrogenic carbon can be abundant in soils as a result of vegetation fires or human applications of biochar purposed for soil fertility improvement, carbon sequestration or contaminant remediation (Paustian et al., 2016; Jones et al., 2019). Its porous structure, large surface area and diverse surface functionality enable it to adsorb many dissolved species such as heavy metals (Kılıc et al., 2013) and natural and contaminant organic compounds (Pignatello et al., 2006; Pignatello et al., 2017). It is expected that biochar can also adsorb various biomolecules, including extracellular enzymes, which is likely to affect the interfacial processes and activities of extracellular enzymes in soils (Sheng et al., 2022). In fact, enzyme adsorption capacity of soils and thermodynamic properties of soil enzyme activity were found to change following biochar addition, and direct biochar adsorption of enzymes is considered a main cause (Keiblinger et al., 2015; Paz-Ferreiro et al., 2015; Elzobair et al., 2016). Considering the critical roles of extracellular enzymes in SOM cycling, it is important to understand the interaction of biochar with enzymes and

* Corresponding author.
E-mail address: rhuang6@albany.edu (R. Huang).

https://doi.org/10.1016/j.geoderma.2024.117082
Received 2 August 2024; Received in revised form 19 October 2024; Accepted 21 October 2024
Available online 31 October 2024

its subsequent impacts on enzyme mobility, activity, and stability.

Depending upon the feedstock and formation conditions, such as temperature and heating duration, biochar can vary greatly in its physicochemical properties, such as aromaticity, specific surface area (SSA), and surface charge (Liu et al., 2015; Xiao et al., 2018). Properties of soil enzymes that may affect their surface adsorption behavior, such as molecular size, surface functional groups and three-dimensional structure, also vary greatly (Bolton, 1997; Shimura, 2000; Kakimoto et al., 2014). Two recent studies tested the impacts of biochar adsorption on enzyme activities and found that different types of biochar adsorbed enzymes to different extents, and therefore inhibited enzyme activity to different extents (Lammirato et al., 2011; Foster et al., 2018). In another study, adsorption capacity of model extracellular pathogenic enzymes (polygalacturonase and cellulase) by biochar made from wood chip and pepper plant wastes were compared (Jaiswal et al., 2018). These studies primarily reported observations of variable enzyme adsorption by biochar, but lacked detailed characterization of relevant enzyme and biochar properties and evaluation of their effects on enzyme adsorption. No studies have quantitatively determined enzyme adsorption capacity of a range of enzymes and biochar types so that the most important controlling factors (biochar properties) and adsorption mechanisms could be determined. Considering the vast diversity of enzymes and biochar types, it is important to fill this knowledge gap so that the effects of fires and biochar addition on soil C cycling can be better understood.

In this work, we explored the mechanisms of enzyme-biochar interaction through batch adsorption of enzymes onto biochars that differ broadly in their major physicochemical properties, as well as enzyme adsorption to soils in the absence and presence of biochar. We hypothesized that the capacity of enzyme adsorption by biochar is controlled by:1) the surface chemistry (i.e. functional groups and surface charge) of both biochar and the enzyme – enzymes with a higher isoelectric point or more protonated surfaces, tend to adsorb more to negatively charged biochar, and 2) by the sizes of enzymes and biochar pores – biochar with more pores of diameters greater than the size of an enzyme is likely to have a larger enzyme adsorption capacity. The biochar samples were made from grass and wood biomass (wheat straw, pine wood sawdust, pine twig, pine bark, and spruce cone) and pyrolyzed at temperature ranging 300 to 600 °C. A wildfire biochar (Jack Pine) was also used as a natural pyrogenic material. Selected biochar samples were oxidized to simulate environmental aging. Four hydrolytic enzymes involved in SOM degradation and differing in molecular weight (α-amylase, urease, protease, and invertase) were selected as model enzymes. Physicochemical properties of the selected biochars and enzymes (e.g., SSA, zeta-potential, and surface functional groups) were characterized. Batch adsorption was performed to quantify the adsorption of enzymes to the studied biochars at different pHs and adsorption isotherms were constructed. Finally, relationships between enzyme adsorption capacities and physicochemical properties of the sorbents and sorbates were examined to evaluate the factors controlling biochar-enzyme adsorption. The relevance of direct biochar adsorption in realistic soil conditions was demonstrated by soil enzyme adsorption experiments using soils with and without biochar of different types. We hypothesized that the effects of biochar presence on soil adsorption of enzymes depend on the relative adsorption capacity of soil and biochar toward an enzyme.

2. Materials and methods

2.1. Reagents and materials

All enzymes used were of high purity from commercial sources. The α-amylase derived from *Aspergilius oryzae*, urease from *Canavalia ensiformis* and invertase from *S. cerevisiae* were purchased from Sigma-Aldrich (St. Louis, MO, USA). Protease from *Aspergillus oryzae* was purchased from TCI (Portland, OR, USA).

2.2. Biochar production

Biochar was synthesized with a procedure described in our previous study (Xu et al., 2016). A range of biomass types, including wheat straw (WS), pine wood sawdust (PW), pitch pine twig (PPT), pitch pine bark (PPB), and Norway spruce cone (SC) were used as the feedstocks. Briefly, biomass was air-dried and shredded into powder (2 – 3 cm pieces for wheat straw). The shredded biomass was tightly packed into glass beakers and covered with aluminum foils, then buried in a bucket filled with sand (>10 cm below surface). The sand bucket was heated in a furnace at 300, 450, or 600°C, with a soaking time of 10 h. The biochars obtained were denoted as 'biomass abbreviation' + 'pyrolysis temperature' (e.g., WS300 for biochar generated from pyrolysis of wheat straw at 300 °C). The biochars obtained were ground into fine powders using a mortar and pestle and passed through a #25 sieve (ϕ = 0.71 mm). A natural biochar sample (large branches that were burned incompletely) was collected from the Altona Jack Pine Barren (Altona, NY) following a wildfire in 2018. The biochar was processed the same way as the lab-made biochar. Several biochar samples were selected for oxidation treatment to simulate the aging of biochar in the environment, to explore its impact on enzyme adsorption. The oxidation treatment followed the method by Sultana *et al.* (Sultana et al., 2011), using a biochar to HNO_3 ratio of 1:4 (w:w) under 104 °C heating for 4 h. The pristine and oxidized biochars were filtered (0.25 μm) and washed repeatedly with deionized water, until no significant UV–vis absorption ($A_{254nm} < 0.01$) was detected in the solution. The washed biochars were lyophilized and used in enzyme experiments.

2.3. Biochar and enzyme characterization

Biochar surface morphology. The specific surface areas (SSA) and pore volume (PV) of biochar were measured at the University of Florida Particle Engineering Research Center on a Quantachrome Autosorb 1, by N_2 and CO_2 gas sorptometry at 77 and 273 K, respectively, which measures pores ≥ 1.3 nm and 0.3 – 1.5 nm diameter (Φ), respectively, according to the theory described by Kwon and Pignatello (Kwon and Pignatello, 2005). Samples were de-gassed under vacuum for at least 18 h at 180 °C prior to analysis. Specific surface area was calculated according to the BET theory using adsorption data in the 0.01–0.3 relative pressure range for N_2 and using grand canonical Monte Carlo simulations of the non-local density functional theory (DFT by Jagiello and Thommes (Jagiello and Thommes, 2004)) for CO_2. Pore volumes and pore size distributions were calculated by DFT theory from the adsorption branch of both N_2 and CO_2 adsorption isotherms.

Zeta potential characterization of biochars and enzymes. Zeta-potentials of both enzymes and biochar were measured on a Malvern Zetasizer (Nano ZS, Malvern Instruments, UK) following the procedure described in a previous study (Malhotra and Coupland, 2004). To obtain the colloidal fraction of the biochars that is suitable for this analysis, about 1 g biochar was thoroughly dispersed in 1 L deionized water. Then the solution was allowed to settle for 24 h and particles remaining in suspension were isolated by membrane filtration. The supernatant was filtered (0.25 μm) and washed repeatedly with deionized water, until no significant UV–vis absorption ($A_{254nm} < 0.01$) was detected in the solution. The colloidal biochars were lyophilized and stored in tightly sealed vials. Enzyme or colloidal biochar solutions (1 – 5 mg·ml^{-1}) were prepared using 10 mM acetate or phosphate buffers at pH 2 to 7. The enzyme or colloidal biochar was mixed in 10 mL centrifuge tubes with 2 mL of 10 mM acetate or phosphate buffers, and the solutions were sonicated for 10 s to ensure thorough suspension. The solutions of enzyme or colloidal biochar were then transferred to a cuvette and placed in a temperature-controlled holder (25 ℃) to measure their electrophoretic mobility. The zeta-potential was calculated from the electrophoretic mobility using the Smoluchowski equation and the data reported are the averages of four measurements.

2.4. Enzyme adsorption experiments

pH edge adsorption experiments. Enzyme adsorption to different biochars was determined across a range of pH conditions. A stock enzyme solution (2 $mg{\cdot}ml^{-1}$) was first prepared by dissolving enzyme powder into 10 mM buffers with pH ranging from 4 to 9. Acetate buffer (10 mM) was used to prepare pH 4 to 5 solutions and phosphate buffer was used for pH 6 to 9. The stock solution was diluted with respective buffers into adsorption working solutions (0.2 $mg{\cdot}ml^{-1}$). Adsorption was conducted in 2 mL centrifuge tubes by mixing 1 mL of enzyme working solution with washed particulate (<0.71 mm) biochar. The amount of biochar added for each enzyme type was adjusted based on the adsorption capacity of the biochar for that specific enzyme. The concentrations used were: α-amylase and protease at 0.2 $mg{\cdot}ml^{-1}$ with 20 $mg{\cdot}ml^{-1}$ biochar, invertase at 0.2 $mg{\cdot}ml^{-1}$ with 15 $mg{\cdot}ml^{-1}$ biochar, and urease at 0.5 $mg{\cdot}ml^{-1}$ with 2.5 $mg{\cdot}ml^{-1}$ biochar. Biochar solutions without enzymes served as controls to measure potential leaching of dissolved organic carbon (DOC) and correct for its interference with enzyme content measurement. The adsorption solutions were thoroughly mixed before placing in a temperature-controlled shaker for 4 h (225 rpm and 25 °C). Preliminary tests showed that adsorption equilibrium was reached within 2 h (data not shown). Following adsorption, the solutions were centrifuged at 40×10^3 *g* for 15 min, and the clear supernatants were transferred into new 2 mL tubes for enzyme concentration analysis. Enzyme concentration in the supernatant was measured using the Bradford Protein Assay (He, 2011) and the amount of enzyme adsorption was calculated as:

$$Enzymeadsorption\left(\frac{mg}{g}\right)=\frac{totaladdedenzyme(mg)-supernatantenzyme(mg)}{totaladdedsolidsorbent(g)}$$

Biochar adsorption isotherms. Adsorption isotherms were constructed using batch adsorption experiments with 1 mL of enzyme working solutions of varying concentrations. The amounts of biochar used were adjusted based on the adsorption capacity of each specific enzyme as described above. The adsorption experiments were conducted at pH 5 using 10 mM acetate buffer. Measurement of enzyme concentrations after adsorption followed the same procedure as described above. The adsorption data were fitted using both Langmuir and Freundlich isotherms (equation#1 and #2 below, respectively), performed in the Origin software (2019b).

$$q_e=\frac{K_L Q_m C_e}{1+K_L C_e} \quad (1)$$

$$q_e=K_f {C_e}^{1/n} \quad (2)$$

Q_m is maximum adsorption capacity, q_e is enzyme adsorption amount at equilibrium, C_e is enzyme concentration at equilibrium, K_L is Langmuir constant, K_f is distribution coefficient, and n is the correction factor.

Soil adsorption experiment. Enzyme adsorption to soils in the absence and presence of biochar was performed. An agricultural soil was used in this experiment, which was collected from a long-term field study of biochar application, located at the Columbia Basin Agriculture Center (CBARC) near Pendleton, Oregon. The Walla Walla silt loam soil (coarse-silty, mixed, superactive, mesic Typic Haploxerolls) with 18 % clay, 70 % silt, and 12 % fine sand (pH = 4.8) was sampled from sites adjacent to the biochar-applied field and its physicochemical properties can be found in Bista *et al.* (Bista et al., 2019). The soil was homogenized and passed through sieve#35 (0.5 mm) to remove particulate organic matter and air dried (for a week), prior to use. The soil was mixed with three biochar types (PW600, WS600, and wildfire pine char) at four rates of 0, 1, 2.5, and 5 wt%, covering the common charcoal C content in agricultural soils and biochar application rates (Skjemstad et al., 2002; Machado et al., 2018). Adsorption was conducted in 2 mL centrifuge tubes by mixing 1 mL of 0.1 mg/mL α-amylase, invertase, protease and 1 mg/mL urease solutions with 500, 200, 200 and 100 mg of soils and soil-biochar mixtures, respectively. The adsorption experiments were conducted at pH 5 using a 10 mM acetate buffer. Adsorption in the absence of biochar addition or enzyme served as control, to determine the baseline of enzyme adsorption and background soil enzyme release. Triplicate experiments were conducted for each treatment. Measurement of enzyme concentrations after adsorption followed the same procedure as described above.

2.5. Data analysis

The relationships between enzyme adsorption capacity and biochar properties were evaluated using linear correlation analyses between maximum adsorption capacities and key biochar properties such as specific surface area and enzyme isoelectric point (IEP). Pearson correlation coefficients were used to determine the strength of these relationships.

To assess the effects of biochar addition on enzyme adsorption, one-way analysis of variance (ANOVA) was performed for each biochar type across the four biochar rates. The significance of differences between the treatments was determined using Tukey's Honest Significant Difference (HSD) test at a significance level of $p < 0.05$. The statistical analyses were performed using JMP software (SAS Institute, Cary, NC).

3. Results and discussion

3.1. Properties of enzyme and pristine biochar

The four enzymes selected, urease, invertase, protease, and α-amylase and, have molecular weights of 640, 270, 67, and 54 kD, respectively (Table S1). Correspondingly, the hydrodynamic diameters of the smallest and largest enzymes (α-amylase and urease) are about 7 nm and 14 nm, respectively (Follmer et al., 2004). Their isoelectric point (IEP), determined by electrophoretic mobility measurement, ranged from 3.0 to 5.0, with that of urease being the greatest and that of protease being the lowest (Table S1 and Fig. 1A).

The biochar samples possessed varying organic components and surface properties. The biochar increased in aromaticity with increasing pyrolysis temperatures and correspondingly decreased in alkyl and O-containing functional groups (Table S2 – S4, Fig. S1). Wheat straw biochar (WS600) had abundant silica (~5% Si) on its surface relative to other biochar samples, as well as higher O content (Table S3). All pristine 600 °C biochar samples had abundant O-containing C functional groups, with O-alkyl groups representing 8.6 to 13.3 % and carboxyl and carbonyl groups each accounting for 2.3 to 5.5 % of surficial C (Table S4).

Zeta-potential measurements showed that the IEP of the biochars ranged from 2.5 to 3.9, indicating that the biochars would remain net negatively charged across the pH range of the adsorption experiments (Table S5 and Fig. 1B). The IEPs of wheat straw biochars were lower than those of pine wood (2.5 to 2.7 compared to 3.5 – 3.9, respectively), which was likely caused by the presence of abundant silica in wheat straw biomass (IEP of silica is about 2). Consistent with previous findings (Suliman et al., 2016), biochar samples produced at temperature below 500°C (WS300, PW300 and PW450) showed low N_2 SSA (<5 $m^2{\cdot}g^{-1}$) and those produced at 600°C possessed larger SSA (most above 200 $m^2{\cdot}g^{-1}$, except SC600) (Table S5). Surface areas measured by CO_2 (180 to 650 $m^2{\cdot}g^{-1}$) were greater than those by N_2 because CO_2 surface area includes pores smaller than 1.5 nm diameter, and similarly increased with increasing pyrolysis temperature. Biochar total pore volume correspondingly increased with pyrolysis temperature. The much larger pore volumes measured by CO_2 than by N_2 for most biochar samples (except for PPB600 and PPT600 that have similar values) suggests that, the great majority of the pore volume was found in pores smaller than 1.5 nm, which are unlikely to be accessible to enzymes considering the dimensions of enzymes (Table S6). However, the

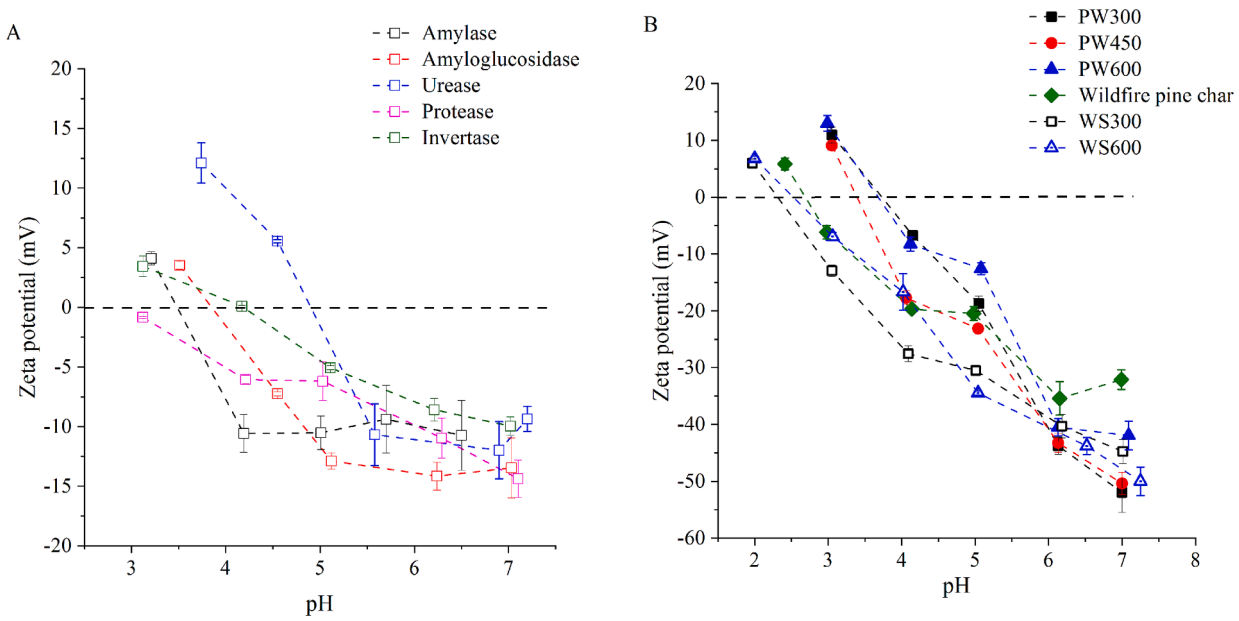

Fig. 1. Zeta potentials of different enzymes (A) and biochar (B) from pH 2 to 7.

proportion of larger enzyme-accessible pores, as measured by N_2, differed between biochar samples. Considering the dimensions of α-amylase (6.8 × 5.3 × 3.6 nm, 54 kDa) (Robert et al., 2003a), the N_2-pore volume was separated into < 5.2 nm and > 5.2 nm portions. The data showed that the majority of pore volume in biochar samples with large pore volumes (most 600 °C chars) was located in pores < 5.2 nm (>88 %), while that of biochars with relatively small pore volumes (all 300 °C, and WS600 and SC600) was located in > 5.2 nm pores (>74 %). This result indicates that the biochar samples possessed different pore size distribution and varying portions of the pores were accessible for enzyme adsorption.

3.2. *Effects of pH on enzyme adsorption to biochar*

Solution pH modulates the protonation and deprotonation of the surface functional groups, and subsequently, net surface charge of the enzymes and biochars (Fig. 1). Adsorption of α-amylase, urease, protease and invertase to different biochar samples over a pH range from 4 to 9 similarly decreased with increasing pH (Fig. 2). Such pH dependency suggests that surface charge was a primary control on enzyme adsorption to biochar and electrostatic interaction was a primary adsorption mechanism. For example, urease showed the greatest pH dependence and also showed the largest decrease in adsorption over the pH range. The enzymes had isoelectric points around pH 3 to 5 and also showed the largest decrease in adsorption over this pH range. Regarding the difference among biochar samples, greater decrease in enzyme adsorption with increasing pH was observed for wildfire pine char than for PW600 and WS600 biochar. This result was possibly related to the difference in surface functionalities and their (de)protonation behaviors.

3.3. *Biochar enzyme adsorption isotherms*

Adsorption isotherms for all the enzymes and biochar combinations tested were best described by the Langmuir model (Fig. 3, Fig. S2 and Table 1), with R^2 always > 0.92. In comparison, fitting with the Freundlich model resulted in most R^2 values less than 0.8, and in some cases, the fitting failed (Fig. 3, and Table S7). Overall, adsorption capacity (Q_m) varied significantly between enzymes, with that of urease ranging between 67 to 232 $mg{\cdot}g^{-1}$ and that of the other enzymes ranging between 0 to 11 $mg{\cdot}g^{-1}$ at pH 5. Adsorption of each enzyme also differed greatly between biochar types, including those of the same feedstock (but different temperatures) and those of the same pyrolysis temperature. For example, adsorption of α-amylase, protease and urease to WS600 was greater than that of PW600, while the opposite was true for invertase. Higher temperature biochars had greater enzyme adsorption capacity than lower temperatures biochars in all combinations tested except in the case of urease adsorption to wheat straw biochar.

Several observations further support the conclusion that electrostatic interaction was the primary adsorption mechanism between negatively charged functional groups on biochar surfaces and positively charged moieties of enzymes. Regardless of the biochar type, urease, the enzyme with the highest IEP, and the only one with a net positive charge at pH 5, showed much greater adsorption than the other enzymes. Protease and α-amylase, the enzymes with the most negative charge, showed the lowest biochar adsorption capacities. The wheat straw biochars (WS300 and WS600) had the lowest IEPs (most net negative surfaces) and also showed the highest enzyme adsorption capacities (except in the case of invertase). Explanations for the variations in enzyme adsorption among the biochars are discussed further below.

3.4. *Effects of oxidation on biochar surface properties and enzyme adsorption*

The high temperature biochars (PW600, WS600, PPB600, PPT600 and SC600) were selected for oxidation treatment to simulate the oxidative aging of biochar in the environment and explore its impact on enzyme adsorption. Characterization of the oxidized biochar and comparison with the pristine biochars showed that biochar properties such as surface elemental composition and functionality and surface charge changed after the oxidation treatment. As shown by the X-ray photoelectron spectroscopy (XPS) and Zeta-potential data, HNO_3 oxidation introduced abundant O-containing functional groups such as carboxylates and carbonyls (Table S3 – S4) and this increased the negative charge on biochar surfaces (Fig. 4A). Surfacial O abundance increased at least two folds after oxidation and the resulting O/C molar ratios increased from about 0.05 to 0.16 – 0.19 (from 0.13 to 0.31 for WS600). The relative abundance of carboxyl groups also increased to 6.7 – 10.3 % after oxidation, compared to about 2.5 % in pristine chars. As a result, IEP of the oxidized biochar decreased to below pH 2.0 and surface density of the negative charges increased (Fig. 4A). Regarding surface morphology, oxidation decreased both total pore volume and SSA of

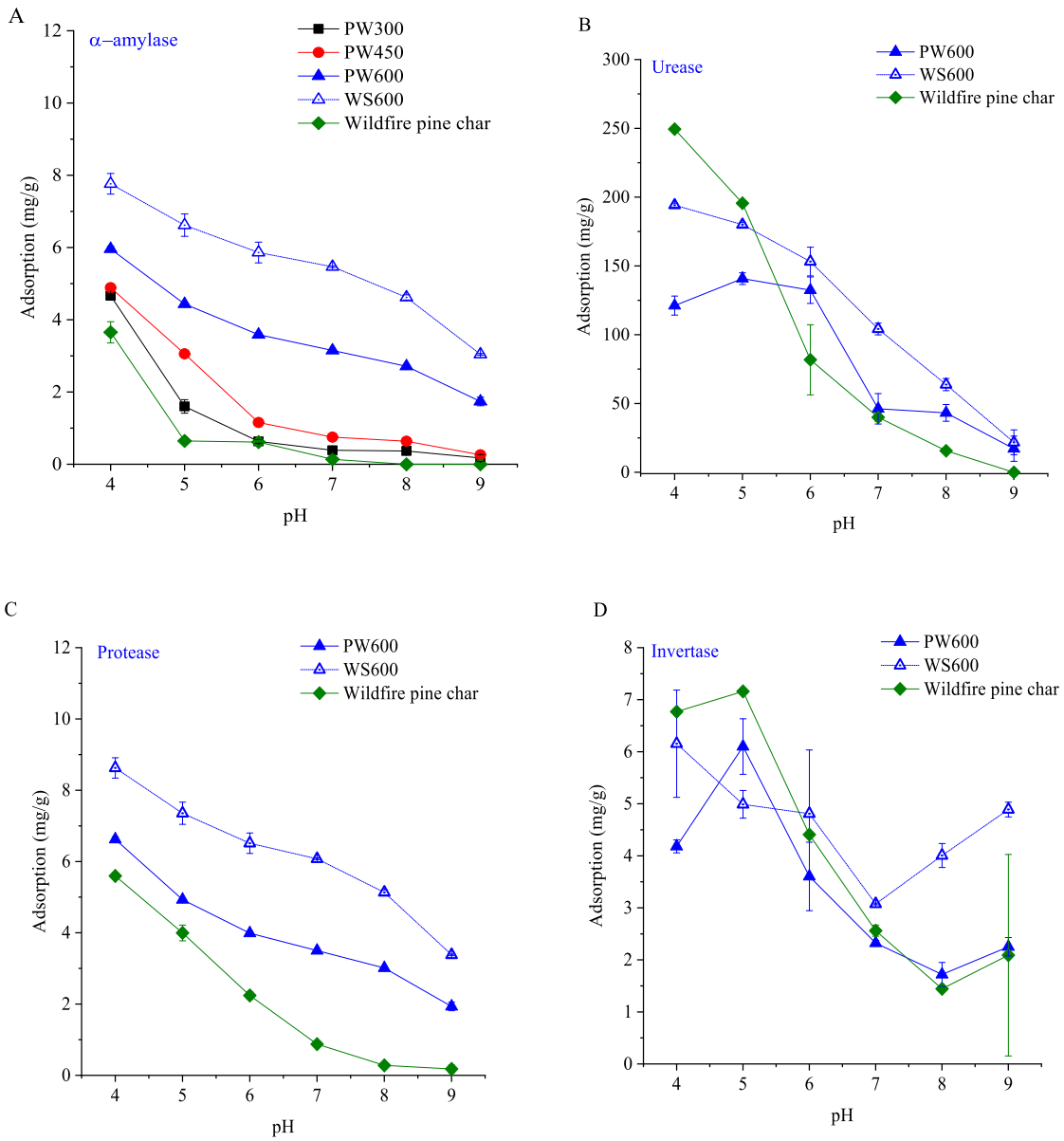

Fig. 2. The adsorption of α-amylase (A), urease (B), protease (C), and invertase (D) onto different biochars from pH 4 to 9. Concentrations used were: α-amylase and protease = 0.2 mg·ml^{-1} with biochar = 20 mg·ml^{-1}; invertase = 0.2 mg·ml^{-1} with biochar = 15 mg·ml^{-1}; urease = 0.5 mg·ml^{-1} with biochar = 2.5 mg·ml^{-1}.

almost all biochars, greatly in the case of N_2-BET (Table S6). This was likely caused by enlargement and merging of pores, as the proportion of < 5.2 nm diameter pores decreased and that of > 5.2 nm pores increased with biochar oxidation in most cases. The exception was WS600 biochar which, upon oxidation treatment, had increased pore volume and larger proportions of smaller nanopores (1.3 – 5 nm) measured by N_2 adsorption. This may have been caused by the relatively high silica content in wheat straw that dissolved during HNO_3 oxidation.

Oxidation of biochar showed varying effects on α-amylase adsorption (Fig. 4B, Fig. S3 and Table 2). Adsorption to WS600 was greatly enhanced after oxidation (90 compared to 6 mg·g^{-1}), while the other biochars showed much smaller increases and PPT600 biochar showed a reduction in maximum adsorption capacity. The mechanism of enzyme adsorption may have changed following biochar oxidation, as suggested by the lower Langmuir constants (K_L) of oxidized biochar compared to those of the corresponding pristine biochars (Table 2). Langmuir constant generally indicates the affinity between sorbate and sorbent surfaces (Tu et al., 2009). Thus, the decrease in the K_L values for oxidized biochar suggest that, though oxidation increased the biochars' net negative charge, the added functional groups, which were predominately carboxylates, may have had a lower enzyme adsorption affinity. The increase of pore volume in WS600 following oxidation may be responsible for the greater enhancement of α-amylase adsorption by this biochar after oxidation. The impacts of surface oxidation are discussed further below.

3.5. *Effects of biochar on soil adsorption of enzymes*

Biochar addition was shown to differentially affect soil adsorption of enzymes, varying with the differences in enzyme adsorption capacity between indigenous soils and biochar (Fig. 6). Addition of PW600 and WS600 significantly enhanced soil adsorption of α-amylase (which increased with increasing biochar addition rate), while wildfire char showed no significant effect (Fig. 6A). The difference between biochar samples corresponds to their adsorption capacity, with wildfire char having the smallest α-amylase adsorption among the three types of biochar (Fig. 2B). In comparison, the effects of biochar addition on invertase and protease adsorption was not significant for most biochar

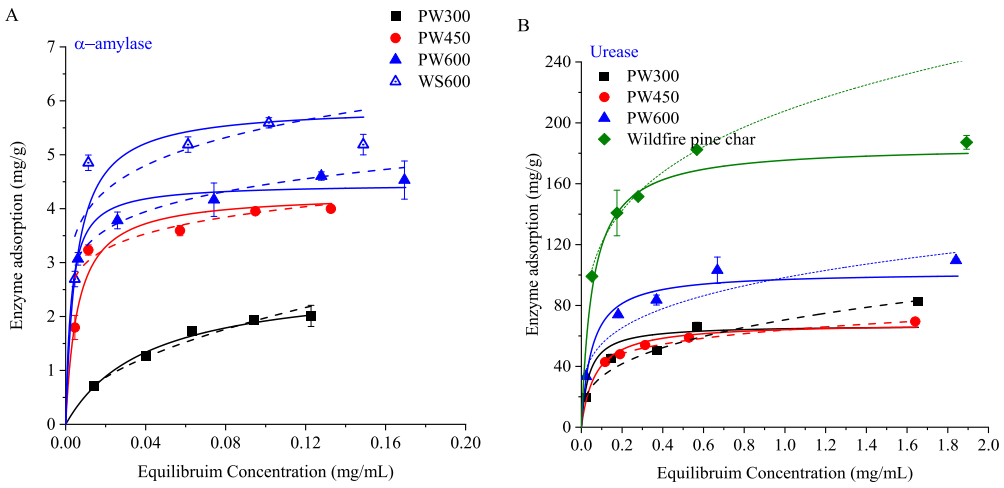

Fig. 3. Adsorption isotherms of α-amylase (A) and urease (B) onto different biochars at pH 5, fitted with both the Langmuir (solid line) and Freundlich (dash line) models.

Table 1
Langmuir fitting parameters for the adsorption of α-amylase, protease, urease and invertase onto different biochars at pH5. Q_m is the maximum adsorption capacity and K_L is the Langmuir constant. NA: not analyzed.

Biochar types	α-amylase			Protease		
	Q_m (mg/g)	K_L (mL/mg)	R^2	Q_m (mg/g)	K_L (mL/mg)	R^2
PW300	2.7	24.5	0.99	NA	NA	NA
PW450	4.3	166.8	0.95	NA	NA	NA
PW600	4.5	373.5	0.98	8.9	26.7	0.92
Wildfire pine char	0.0	0.0	–	8.5	9.2	0.95
WS300	0.0	0.0	–	NA	NA	NA
WS600	5.9	188.9	0.91	11.5	20.7	0.95
	Urease			Invertase		
	Q_m (mg/g)	K_L (mL/mg)	R^2	Q_m (mg/g)	K_L (mL/mg)	R^2
PW300	67.1	21.3	0.97	NA	NA	NA
PW450	68.5	14.6	0.96	NA	NA	NA
PW600	102.0	19.6	0.98	7.4	56.5	0.99
Wildfire pine char	185.2	18.0	0.97	25.0	10.2	0.96
WS300	232.6	14.3	0.93	NA	NA	NA
WS600	169.1	3.9	0.99	4.7	176.1	0.98

treatments, except for the wildfire char on invertase and WS600 on protease at the highest rates (Fig. 6B and 6C). The addition of WS600 biochar at a 5 % rate enhanced protease adsorption by the soil, as WS600 demonstrated higher adsorption capacity for protease compared to PW biochar in previous isotherm results (Table 1). The addition of PW600 and WS600 slightly enhanced urease adsorption by the soil, with WS600 showing greater enhancement (Fig. 6D), due to the higher adsorption capacities of WS600 than PW600 toward urease. The difference in biochar effect among enzymes is related to their different affinities for the untreated soil and added biochar. Because the tested soil showed significantly greater adsorption of urease (~9.8 mg/g), invertase and protease (~0.25 mg/g) than α-amylase (no detectable adsorption) at the test condition, the effect of biochar addition on the adsorption of these three enzymes was not as pronounced as the effect on α-amylase.

A previous study reported that addition of biochar derived from wood chips, vineyard pruning, and wheat straw reduced the adsorption of bovine serum albumin to a sandy loam soil (bovine serum albumin adsorption to biochar was not measured) [12]. Results from this work suggest that the effects of biochar on soil adsorption of enzymes depend on the relative affinity of an enzyme toward soil and biochar. When a soil has a weak affinity for an enzyme and biochar has relatively greater affinity, biochar addition may enhance enzyme adsorption.

3.6. Mechanisms of enzyme-biochar interactions

Following their release by microbes, enzymes are subjected to multiple interacting pedological and climatic factors that affect their mobility, activity, and activity lifetime (stability) in soils. For example, enzymes can be degraded by proteases (Schimel et al., 2017) or denatured by heat and drought, while mineral adsorption can enhance the resistance of enzymes to the degradation and denaturation stress (Ensminger and Gieseking, 1942). The addition of biochar represents a change to soil pedological properties that may interact with other environmental factors in affecting the mobility, activity, and stability of enzymes.

This study explored the mechanisms of biochar and enzyme interactions by testing a diversity of enzymes and biochars that differed in key physicochemical properties. pH-edge adsorption experiments suggested that enzyme adsorption to biochar was primarily driven by electrostatic interaction because of correspondences between isoelectric points of enzymes and biochars and changes in adsorption capacity (Figs. 1 and 2). All adsorption isotherms were best fit by the Langmuir isotherm, regardless of enzyme or biochar types. This suggests that the enzyme adsorption occurred as a monolayer on biochar surfaces. Enzymes are amphiphilic and can simultaneously possess charged, neutral, and nonpolar moieties that enable them to sorb onto various substrates, depending on their surface chemistry (Six and Dennis, 2000; Manavalan et al., 2015). Biochar surfaces consist of various O-containing functional groups (e.g., carboxylate and phenolic groups) that carry negative charges even at very low pHs (Lee et al., 2010; Mukherjee et al., 2011). At the tested pH of 5, although both enzyme and biochar were net negatively charged (i.e., abundant deprotonated moieties), the positively charged moieties of the enzymes can bind to biochar O-containing groups.

Considering the vast diversity of enzymes and biochars, it is also important to understand how enzyme adsorption may be affected by key enzyme and biochar properties beside surface charge. First, enzyme adsorption capacity of biochar may be partly controlled by its surface morphology that dictates the accessibility of enzymes to biochar's surface. Plots of enzyme adsorption capacity versus biochar BET SSA show that, while adsorption of α-amylase was directly related to biochar N_2 SSA, there was no clear relationship between urease adsorption and SSA (Fig. 5A and 5B). In addition, the correlation between α-amylase adsorption and N_2 SSA was better than that with CO_2 SSA. The data suggest the relevance of enzyme size and biochar porous structure in

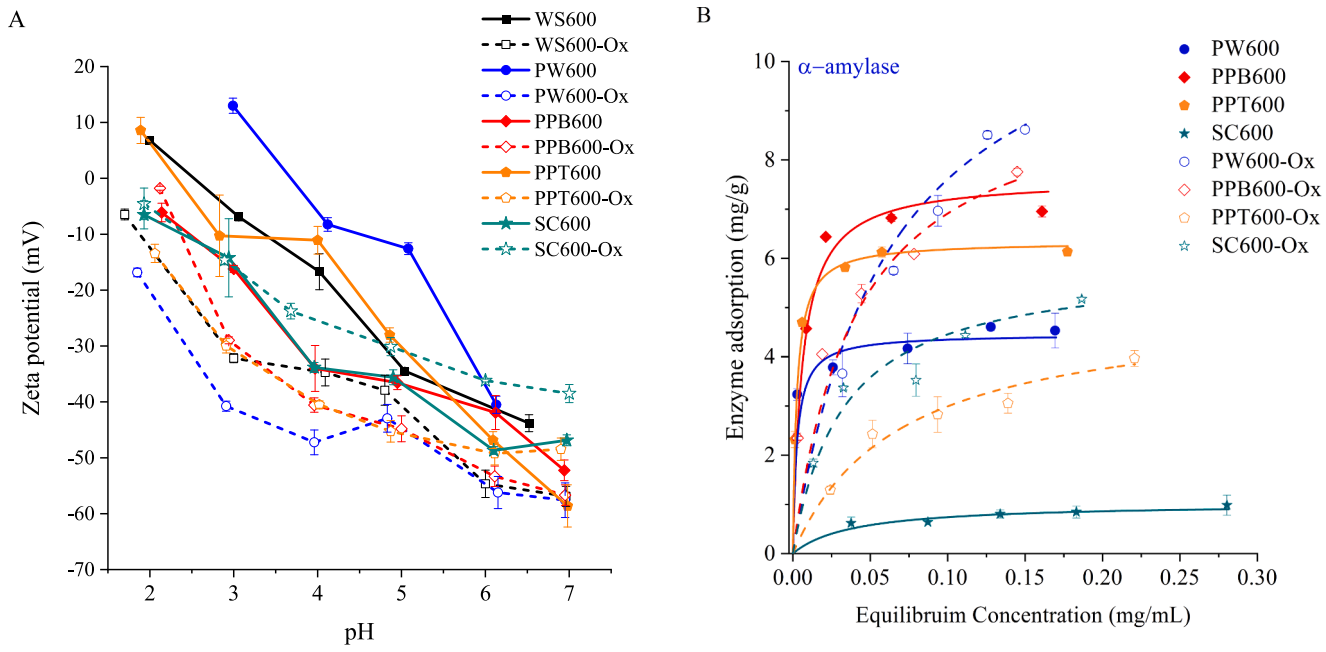

Fig. 4. Comparison of the Zeta-potential of biochars from pH 2 to 7 (A) and adsorption isotherms of α-amylase onto biochars at pH 5 (B) before and after HNO_3 oxidation.

enzyme adsorption, because enzyme size determines the accessibility and contribution of biochar surface pores in enzyme adsorption. Since α-amylase is the smallest enzyme, it was able to access more of the biochar surface, while urease, due to its larger molecular weight and size, can access less biochar surface (and pores). Biochar is a porous material with a wide range of pore sizes (Brewer et al., 2014), including micropores (<2 nm diameter) that account for the most pore space (>50 %) (Muzyka et al., 2023). Molecular dimensions of enzyme can range from 2 to 10 s of nanometers (Codding et al., 1974; Jabri et al., 1995; Robert et al., 2003b). Previous work showed that proteins were restricted from adsorption to surfaces within pores less than twice their size (Zimmerman et al., 2004). This explains the poor relationship between SSA and adsorption of the larger enzyme, urease. Because CO_2 SSA has a large contribution from < 1.5 nm pores that are unlikely to contribute to enzyme adsorption, CO_2 SSA showed a poorer correlation than N_2 SSA with enzyme adsorption amount.

Second, the chemistry of biochar and enzyme surface can affect both enzyme binding affinity and sorption capacity, because enzyme adsorption was driven primarily by electrostatic interaction. This is first reflected in the general increase in adsorption with enzyme molecular weight and ratio between sorbate and sorbent isoelectric point (Fig. 5C and 5D). Urease, with the largest molecular weight (640 kDa) and highest IEP (5.0) showed the greatest adsorption to biochar, because it has the greatest number of positively charged functional groups to interact with biochar's negatively charged surface. Other enzymes with relatively low IEP had predominantly deprotonated surfaces at the experimental pH (5.0), thus were repulsed by the biochar surface. The importance of surface chemistry was also manifested in the result of the biochar oxidation experiment. After biochar's surface became more oxidized and more negatively charged, enzyme affinity (K_L) to biochar became weaker as a result of increasing electrostatic repulsion (Fig. 4B and Table 2).

It is worth noting that enzyme adsorption to porous material such as biochar could involve the interplay of multiple processes and factors beyond what were analyzed herein. For example, although electrostatic interaction is the primary driving force, hydrophobic interaction may also contribute to enzyme adsorption, since biochar is known to have varying degrees of hydrophobicity and enzymes may have surface hydrophobic moieties as well (Kellis et al., 1988; Tilton et al., 1991; Gray et al., 2014). This could mask the relative importance of electrostatic interaction in enzyme adsorption. In addition, properties of biochar are highly variable and do not change consistently with temperatures or across biomass types. For example, although oxidation similarly added O-containing functional groups to biochar surfaces, the change varied with biomass type, as did changes to biochar surface morphology. Therefore, it is understandable that enzyme adsorption cannot be explained by individual factor such as molecular weight, biochar surface area, or surface charge, as analyzed herein.

The soil enzyme adsorption result demonstrated the relevance and potential contribution of direct biochar adsorption of enzymes in soils. Therefore, biochar amendment can affect the spatial distribution and mobility of enzymes in soils by direct adsorption on biochar, while the effect (enhancement or reduction) depends on the relative enzyme adsorption capacity on the soil and biochar (Fig. 6). Although extensive studies have been devoted to measuring the responses of soil enzymes to biochar addition, variations among enzymes and biochar were observed and await reconciliation (Pokharel et al., 2020; Liao et al., 2022). Although microbial production intrinsically regulates the quantity of enzymes in soils, this work underlines the needs to consider direct enzyme-biochar interaction in evaluating the dynamics of soil enzyme activity (depends on both the quantity and the forms of enzymes in soils) and the effects on soil C and nutrient cycling.

4. Conclusions and implications

The mobility and activity of extracellular enzymes in soil is largely controlled by their interaction with other soil physical components, and therefore controls microbial SOM decomposition. This work improves current understanding of enzyme-biochar interactions, through systematic characterization of enzyme adsorption for a diversity of biochar and enzyme types. Our findings suggest that both surface chemistry and pore structure of biochar are important in controlling the mechanism and capacity of enzyme adsorption by pyrogenic organic matter. Specifically:

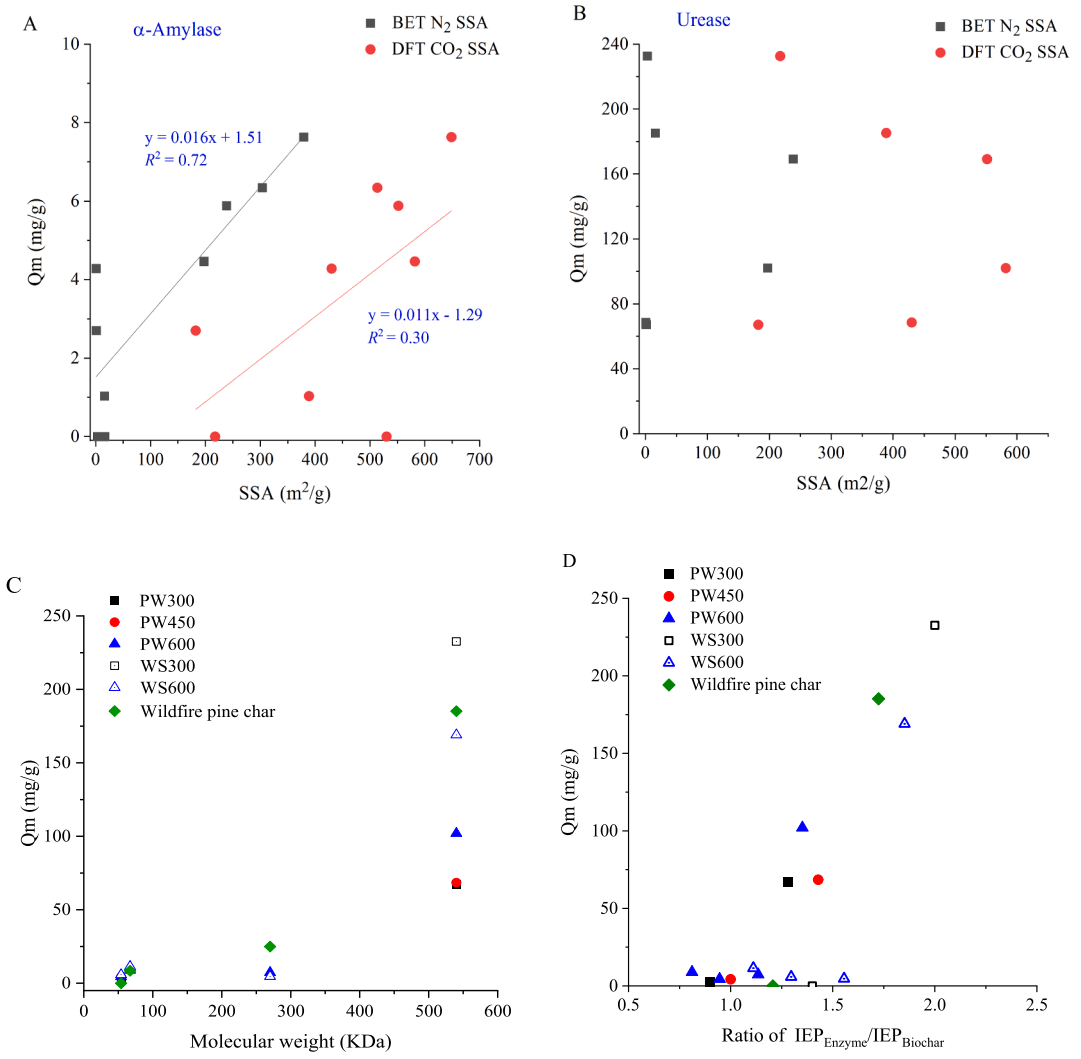

Fig. 5. Relationships between enzyme adsorption capacities biochar and enzyme properties; α-amylase (A) and urease (B) adsorption capacity versus N_2-BET and CO_2-DFT specific surface area, enzyme adsorption capacity versus enzyme molecular weights (C), and enzyme adsorption capacity versus enzymes/biochar isoelectric point ratios (D).

1) Enzyme adsorption onto biochar is mainly driven by electrostatic interaction, likely between positively charged moieties of enzymes and negatively charged biochar surface functional groups at common environmental pH conditions;
2) While surface charge is the primary control on biochar enzyme adsorption, porous structure of biochar is important in modulating enzyme adsorption capacity. Because a significant portion of biochar pores are comparable or smaller than the sizes of enzymes, those pores are not accessible to enzymes and are not available for enzyme adsorption, particularly for large enzymes.
3) Surface oxidation of biochar, such as would occur with aging, leads to greater enzyme adsorption in most cases due to the addition of O-containing functional groups, but also weaker enzyme affinity as a result of enhanced charge repulsion and changes in functional group type distribution. However, the effects on enzyme adsorption capacity also depend on how oxidation affects the surface porous structure of biochar, because these changes varied with biomass types.
4) Biochar addition can change soil adsorption of enzymes that can be enhanced or reduced, depending on the relative affinity of soil and biochar toward an enzyme. The direct biochar-enzyme interaction can affect the mobility and activity of enzymes in soils.

While many studies have sought to determine the rates and controls of mineralization of pyrogenic organic matter or various kinds, there has been surprisingly little discussion of the reasons behind its great persistence. When it is discussed, it is most often attributed to chemical recalcitrance, specifically, condensed aromatic content (Zimmerman, 2010; Luo et al., 2023). Another potential mechanism that should be more widely considered is the adsorption and inactivation of microbial enzymes. The findings of this study on enzyme adsorption to biochars should be extended to explore the impacts of biochar adsorption on enzyme activity, and further, on its influence on the persistence of pyrogenic organic matter.

The mechanistic understanding developed here will help predict the impacts of biochar on enzyme mobility in soil and guide future studies on the effects of biochar on enzyme activity and therefore, soil C cycling. Considering the current and future increases in landscape fires due to climate change, and growing interests in purposeful biochar application to agricultural soils as a means of fighting climate change, these types of studies will be critical.

Authors contributions

Zeng performed experiments, analyzed data, and wrote the paper,

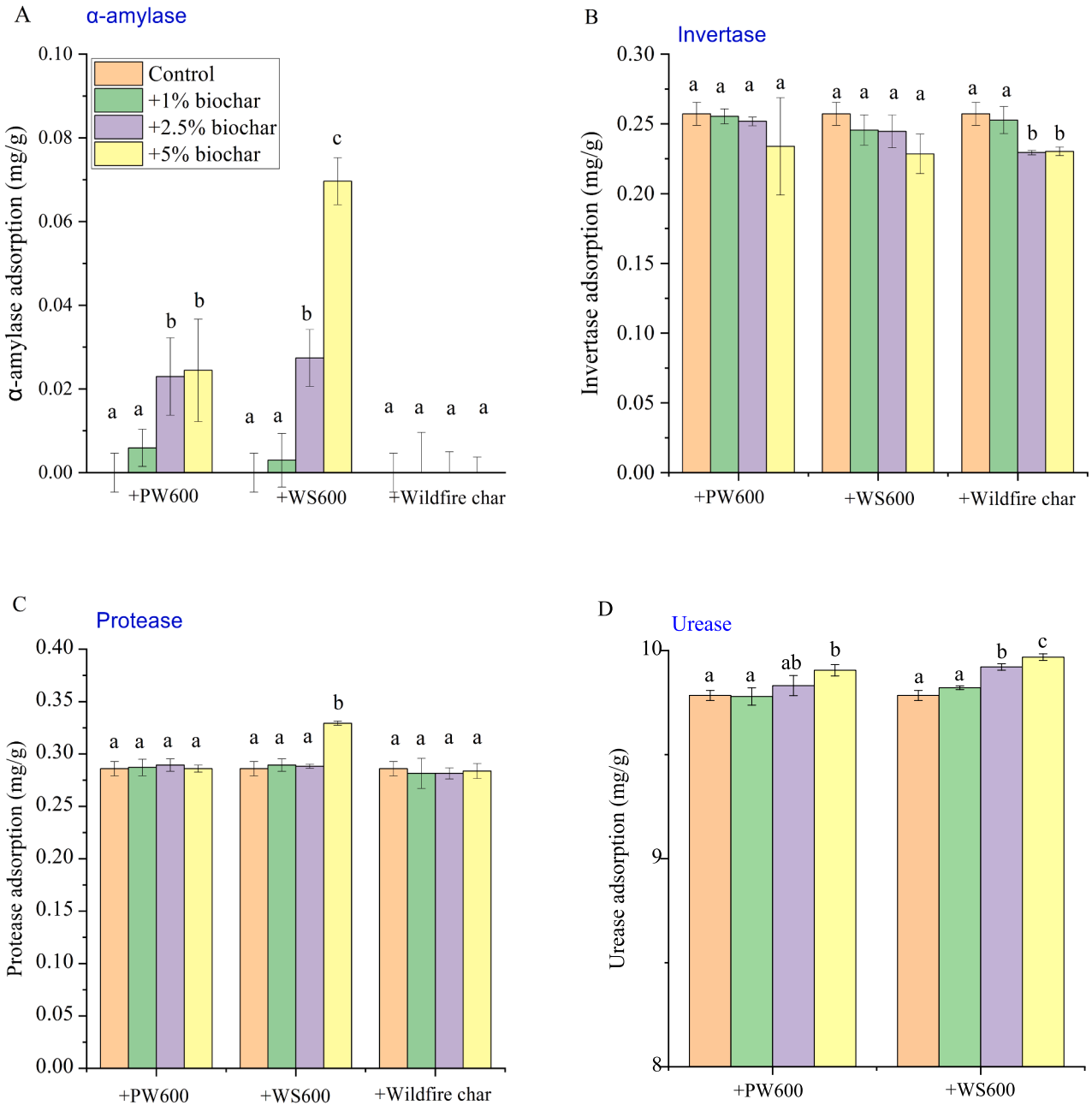

Fig. 6. Enzyme adsorption by a silt loam soil mixed with three types of biochar, each at four rates of 0, 1, 2.5, and 5 wt%. The data were shown as mean ± standard deviation ($n = 3$). The effects of biochar addition on enzyme adsorption at the four biochar rates (within the same biochar type) was tested with the one-way ANOVA (Tukey test), and significant difference ($p < 0.05$) among the treatments were indicated with different letters.

Table 2
Langmuir fitting parameters for the adsorption of α-amylase onto different biochars with/without chemical oxidation at pH5.

Biochar types	Pristine			Oxidized		
	Q_m (mg/g)	K_L (mL/mg)	R^2	Q_m (mg/g)	K_L (mL/mg)	R^2
PW600	4.46	373.5	0.98	12.28	16.3	0.95
WS600	5.88	188.9	0.91	90.36	6.1	0.91
PPB600	7.63	163.9	0.99	9.74	24.5	0.99
PPT600	6.34	394.5	0.99	5.04	14.6	0.97
SC600	1.03	25.9	0.92	5.90	30.8	0.97

Huang conceived the idea and wrote the paper, and Zimmerman performed experiments and wrote the paper.

CRediT authorship contribution statement

Lingqun Zeng: Writing – original draft, Methodology, Investigation, Formal analysis, Data curation, Conceptualization. **Andrew R. Zimmerman:** Writing – review & editing, Data curation. **Rixiang Huang:** Writing – review & editing, Supervision, Resources, Funding acquisition, Conceptualization.

Funding

This work was supported by National Science Foundation (#2120547), US Department of Agriculture – National Institute of Food and Agriculture (NIFA) (#2022-67020-36123), and Startup funds from University at Albany.

Declaration of competing interest

The authors declare that they have no known competing financial interests or personal relationships that could have appeared to influence the work reported in this paper.

Acknowledgements

We thank Dr. Mark Lesser at SUNY-Plattsburgh for collecting charcoal samples from the July 2018 Altona wildfire. We thank Salimar Cordero at University of Massachusetts at Amherst for assisting the zeta-potential measurement of biochar samples. We also thank Drs. Larry Pritchett and Stephen Machado at Oregon State University for providing the agricultural soil used in this work.

Appendix A. Supplementary data

Carbon structure quantified by ^{13}C NMR and surface elemental contents and functionalities determined by XPS. Surface morphology characterized by gas sorptometry. Deconvoluted XPS spectra (C_{1S}) and enzyme adsorption isotherms for different biochars. Supplementary data to this article can be found online at https://doi.org/10.1016/j.geoderma.2024.117082.

Data availability

Data will be made available on request.

References

Allison, S.D., 2006. Soil minerals and humic acids alter enzyme stability: implications for ecosystem processes. Biogeochemistry 81, 361–373.
Bista, P., Ghimire, R., Machado, S., Pritchett, L., 2019. Biochar Effects on Soil Properties and Wheat Biomass vary with Fertility Management. Agronomy-Basel 9.
Bolton, D.J., Kelly, C.T., Fogarty, W.M., 1997. Purification and characterization of the amylase of bacillus flavothermus. Enzyme Microb. Technol. 20, 340–343.
Brewer, C.E., Chuang, V.J., Masiello, C.A., Gonnermann, H., Gao, X., Dugan, B., Driver, L. E., Panzacchi, P., Zygourakis, K., Davies, C., 2014. New approaches to measuring biochar density and porosity. Biomass Bioenergy 66, 176–185.
Burns, R.G., DeForest, J.L., Marxsen, J., Sinsabaugh, R.L., Stromberger, M.E., Wallenstein, M.D., Weintraub, M.N., Zoppini, A., 2013. Soil enzymes in a changing environment: Current knowledge and future directions. Soil Biol. Biochem. 58, 216–234.
Codding, P.W., Delbaere, L.T., Hayakawa, K., Hutcheon, W.L., James, M.N., Jurásek, L., 1974. The 4.5 Angstrom resolution structure of a bacterial serine protease from Streptomyces griseus. Can J Biochem 52, 208–220.
Elzobair, K.A., Stromberger, M.E., Ippolito, J.A., 2016. Stabilizing effect of biochar on soil extracellular enzymes after a denaturing stress. Chemosphere 142, 114–119.
Ensminger, L., Gieseking, J., 1942. Resistance of clay-adsorbed proteins to proteolytic hydrolysis. Soil Sci 53, 205–210.
Follmer, C., Pereira, F.V., da Silveira, N.P., Carlini, C.R., 2004. Jack bean urease (EC 3.5.1.5) aggregation monitored by dynamic and static light scattering. Biophys. Chem. 111, 79–87.
Foster, E., Fogle, E., Cotrufo, M., 2018. Sorption to Biochar Impacts β-Glucosidase and Phosphatase Enzyme Activities. Agriculture 8, 158.
Gray, M., Johnson, M.G., Dragila, M.I., Kleber, M., 2014. Water uptake in biochars: The roles of porosity and hydrophobicity. Biomass Bioenergy 61, 196–205.
He, F., 2011. Bradford protein assay. Bio-Protocol e45–e.
Jabri, E., Carr, M.B., Hausinger, R.P., Karplus, P.A., 1995. The Crystal-Structure of Urease from Klebsiella-Aerogenes. Science 268, 998–1004.
Jagiello, J., Thommes, M., 2004. Comparison of DFT characterization methods based on N2, Ar, CO2, and H2 adsorption applied to carbons with various pore size distributions. Carbon 42, 1227–1232.
Jaiswal, A.K., Frenkel, O., Tsechansky, L., Elad, Y., Graber, E.R., 2018. Immobilization and deactivation of pathogenic enzymes and toxic metabolites by biochar: A possible mechanism involved in soilborne disease suppression. Soil Biol Biochem 121, 59–66.
Jones, M.W., Santín, C., van der Werf, G.R., Doerr, S.H., 2019. Global fire emissions buffered by the production of pyrogenic carbon. Nat. Geosci. 12, 742–747.
Kaiser, C., Koranda, M., Kitzler, B., Fuchslueger, L., Schnecker, J., Schweiger, P., Rasche, F., Zechmeister-Boltenstern, S., Sessitsch, A., Richter, A., 2010. Belowground carbon allocation by trees drives seasonal patterns of extracellular enzyme activities by altering microbial community composition in a beech forest soil. New Phytol. 187, 843–858.
Kakimoto, S., Sumino, Y., ichi Akiyama, S., Nakao, Y., 2014. Purification and Characterization of Acid Urease fromLactobacillus reuteri. Agricultural and Biological Chemistry 53, 1119-1125.
Keiblinger, K.M., Liu, D., Mentler, A., Zehetner, F., Zechmeister-Boltenstern, S., 2015. Biochar application reduces protein sorption in soil. Org Geochem. 87, 21–24.
Kellis, J.T., Nyberg, K., Šail, D.a., Fersht, A.R., 1988. Contribution of hydrophobic interactions to protein stability. Nature 333, 784-786.
Kılıc, M., Kırbıyık, C., Çepelioğullar, Ö., Pütün, A.E., 2013. Adsorption of heavy metal ions from aqueous solutions by bio-char, a by-product of pyrolysis. Appl. Surf. Sci. 283, 856–862.
Kwon, S., Pignatello, J.J., 2005. Effect of natural organic substances on the surface and adsorptive properties of environmental black carbon (char): Pseudo pore blockage by model lipid components and its implications for N-probed surface properties of natural sorbents. Environ Sci Technol 39, 7932–7939.
Lammirato, C., Miltner, A., Kaestner, M., 2011. Effects of wood char and activated carbon on the hydrolysis of cellobiose by beta-glucosidase from Aspergillus niger. Soil Biol Biochem 43, 1936–1942.
Lee, J.W., Kidder, M., Evans, B.R., Paik, S., Buchanan Iii, A.C., Garten, C.T., Brown, R.C., 2010. Characterization of Biochars Produced from Cornstovers for Soil Amendment. Environ Sci Technol 44, 7970–7974.
Liao, X.L., Kang, H., Haidar, G., Wang, W.F., Malghani, S., 2022. The impact of biochar on the activities of soil nutrients acquisition enzymes is potentially controlled by the pyrolysis temperature: A meta-analysis. Geoderma 411.
Liu, W.-J., Jiang, H., Yu, H.-Q., 2015. Development of biochar-based functional materials: toward a sustainable platform carbon material. Chem. Rev. 115, 12251–12285.
Luo, L., Wang, J., Lv, J., Liu, Z., Sun, T., Yang, Y., Zhu, Y.-G., 2023. Carbon Sequestration Strategies in Soil Using Biochar: Advances, Challenges, and Opportunities. Environ Sci Technol 57, 11357–11372.
Machado, S., Awale, R., Pritchett, L., Rhinhart, K., 2018. Alkaline biochar amendment increased soil pH, carbon, and crop yield. Crops and Soils 51, 38–39.
Malhotra, A., Coupland, J.N., 2004. The effect of surfactants on the solubility, zeta potential, and viscosity of soy protein isolates. Food Hydrocoll. 18, 101–108.
Manavalan, T., Manavalan, A., Heese, K., 2015. Characterization of lignocellulolytic enzymes from white-rot fungi. Curr Microbiol 70, 485–498.
Mukherjee, A., Zimmerman, A.R., Harris, W., 2011. Surface chemistry variations among a series of laboratory-produced biochars. Geoderma 163, 247–255.
Muzyka, R., Misztal, E., Hrabak, J., Banks, S.W., Sajdak, M., 2023. Various biomass pyrolysis conditions influence the porosity and pore size distribution of biochar. Energy 263, 126128.
Paustian, K., Lehmann, J., Ogle, S., Reay, D., Robertson, G.P., Smith, P., 2016. Climate-smart soils. Nature 532, 49–57.
Paz-Ferreiro, J., Fu, S.L., Mendez, A., Gasco, G., 2015. Biochar modifies the thermodynamic parameters of soil enzyme activity in a tropical soil. J Soil Sediment 15, 578–583.
Pignatello, J.J., Kwon, S., Lu, Y., 2006. Effect of natural organic substances on the surface and adsorptive properties of environmental black carbon (char): attenuation of surface activity by humic and fulvic acids. Environ. Sci. Tech. 40, 7757–7763.
Pignatello, J.J., Mitch, W.A., Xu, W., 2017. Activity and Reactivity of Pyrogenic Carbonaceous Matter toward Organic Compounds. Environ. Sci. Tech. 51, 8893–8908.
Pokharel, P., Ma, Z.L., Chang, S.X., 2020. Biochar increases soil microbial biomass with changes in extra- and intracellular enzyme activities: a global meta-analysis. Biochar 2, 65–79.
Robert, X., Haser, R., Gottschalk, T.E., Ratajczak, F., Driguez, H., Svensson, B., Aghajari, N., 2003. The structure of barley α-amylase isozyme 1 reveals a novel role of domain C in substrate recognition and binding: a pair of sugar tongs. Structure 11, 973–984.
Schimel, J., Becerra, C.A., Blankinship, J., 2017. Estimating decay dynamics for enzyme activities in soils from different ecosystems. Soil Biol. Biochem. 114, 5–11.
Sheng, Y., Dong, H., Coffin, E., Myrold, D., Kleber, M., 2022. The Important Role of Enzyme Adsorbing Capacity of Soil Minerals in Regulating β-Glucosidase Activity. Geophysical Research Letters 49, e2021GL097556.
Shimura, K., Zhi, W., Matsumoto, H., Kasai, K.I., 2000. Accuracy in the determination of isoelectric points of some proteins and a peptide by capillary isoelectric focusing: utility of synthetic peptides as isoelectric point markers. Anal. Chem. 72, 4747–4757.
Sinsabaugh, R.L., Lauber, C.L., Weintraub, M.N., Ahmed, B., Allison, S.D., Crenshaw, C., Contosta, A.R., Cusack, D., Frey, S., Gallo, M.E., Gartner, T.B., Hobbie, S.E., Holland, K., Keeler, B.L., Powers, J.S., Stursova, M., Takacs-Vesbach, C., Waldrop, M. P., Wallenstein, M.D., Zak, D.R., Zeglin, L.H., 2008. Stoichiometry of soil enzyme activity at global scale. Ecol. Lett. 11, 1252–1264.
Six, D.A., Dennis, E.A., 2000. The expanding superfamily of phospholipase A2 enzymes: classification and characterization. Biochimica et Biophysica Acta (BBA)-Molecular Cell Biology of Lipids 1488, 1-19.
Skjemstad, J.O., Reicosky, D.C., Wilts, A.R., McGowan, J.A., 2002. Charcoal carbon in US agricultural soils. Soil Sci. Soc. Am. J. 66, 1249–1255.
Suliman, W., Harsh, J.B., Abu-Lail, N.I., Fortuna, A.M., Dallmeyer, I., Garcia-Perez, M., 2016. Influence of feedstock source and pyrolysis temperature on biochar bulk and surface properties. Biomass Bioenerg 84, 37–48.

Sultana, N., Ikeya, K., Watanabe, A., 2011. Partial Oxidation of Char to Enhance Potential Interaction With Soil. Soil Sci 176, 495–501.
Tilton, R.D., Robertson, C.R., Gast, A.P., 1991. Manipulation of hydrophobic interactions in protein adsorption. Langmuir 7, 2710–2718.
Tu, M., Pan, X., Saddler, J.N., 2009. Adsorption of Cellulase on Cellulolytic Enzyme Lignin from Lodgepole Pine. J Agr Food Chem 57, 7771–7778.
Xiao, X., Chen, B., Chen, Z., Zhu, L., Schnoor, J.L., 2018. Insight into Multiple and Multilevel Structures of Biochars and Their Potential Environmental Applications: A Critical Review. Environ. Sci. Tech. 52, 5027–5047.
Xu, S., Adhikari, D., Huang, R., Zhang, H., Tang, Y., Roden, E., Yang, Y., 2016. Biochar-Facilitated Microbial Reduction of Hematite. Environ Sci Technol 50, 2389–2395.
Zimmerman, A.R., 2010. Abiotic and Microbial Oxidation of Laboratory-Produced Black Carbon (Biochar). Environ Sci Technol 44, 1295–1301.
Zimmerman, A.R., Goyne, K.W., Chorover, J., Komarneni, S., Brantley, S.L., 2004. Mineral mesopore effects on nitrogenous organic matter adsorption. Org Geochem 35, 355–375.